Pramana – J. Phys. (2026) 100:121
https://doi.org/10.1007/s12043-026-03170-z

Controlled remote implementation of operator via non-maximal hyperentanglement and its relevance

CAO THI BICH[1,*] and NGUYEN BA AN[2]

[1]Institute of Physics, Vietnam Academy of Science and Technology (VAST), 10 Dao Tan, Giang Vo, Hanoi, Vietnam
[2]Thang Long Institute of Mathematics and Applied Sciences (TIMAS), Thang Long University (TLU), Nghiem Xuan Yem, Dinh Cong, Hanoi, Vietnam

*Corresponding author. E-mail: ctbich@iop.vast.vn

MS received 2 January 2026; revised 13 April 2026; accepted 29 April 2026
© The Author(s), under exclusive licence to Indian Academy of Sciences 2026

Abstract. Controlled remote implementation of an operator (CRIO) is a global quantum protocol for executing an unknown unitary operator on a distant, unknown quantum state under the control of a remote controller, using a quantum resource shared in advance between the implementers and the controller. One implementer (Alice) has a photon in an unknown state to everyone. The other implementer (Bob) has a general unitary operator that he can execute, but no one else can. The controller (Charlie) does not need to know the explicit forms of both Alice's state and Bob's operator, but reserves the right to decide when the CRIO completes, i.e., when the remote implementation of Bob's operator on Alice's state is complete. Such protocols are fundamentally needed for controllable, scalable quantum distributed computing and cloud-based applications across remote nodes within a quantum network. In this paper, we extend our work (An and Bich, *J. Phys. A: Math. Theor.* **55**, 225307 (2022)), in which a maximally hyperentangled state was used as the quantum resource, to the case of non-maximal hyperentanglement. The parameters identifying the non-maximally hyperentangled state of the quantum resource are deliberately configured to be known exclusively to the controller, ensuring a high level of security. We show that, although the shared hyperentangled state is non-maximal, the controller can still effectively govern the CRIO protocol, achieving unit fidelity at the expense of a finite success probability. This success probability is proportional to the degree of entanglement of the quantum resource, which can be flexibly tuned by appropriate channel engineering. Furthermore, we derive the average fidelity of classical remote implementation of the operator and calculate the average non-conditioned fidelity of the quantum CRIO without the controller's participation. Then we evaluate the relevance of the quantum protocol in terms of the so-called quantumness power and the controller's power.

Keywords. Controlled remote implementation of operator; non-maximal hyperentanglement; quantumness power; controller's power.

PACS Nos **03.67.-a; 03.65.Ud; 03.67.Hk**

Published online: 06 August 2026

1. Introduction

Quantum entanglement [1] is a fundamental phenomenon in quantum physics where the states of two or more particles are weirdly correlated in a way that can by no means happen in classical physics. This leads to what is often referred to as 'spooky action at a distance' [2], implying a measurement of one particle instantaneously influences the state of the others, regardless of the distance between them. Hyperentanglement [3,4] extends the entanglement concept to multiple degrees of freedom (DOFs) simultaneously. Recent research has increasingly focused on hyperentanglement, highlighting its significant potential in quantum information processing and quantum computing, thanks to its enhanced capacity of encoding and processing information, as well as boosting the security level of quantum protocols in the sense that the transmitted information is harder to be intercepted or tampered by unauthorized parties [5–18]. One key application of entanglement is quantum teleportation [19], which enables the transmission of quantum information from one location to another without physically sending the system that carries it. When hyperentanglement is employed, quantum teleportation utilizes multiple DOFs simultaneously, such as polarization DOF (P-DOF) and spatial-path DOF (S-DOF), thereby enhancing the transmission of complex information and improving the efficiency of quantum communication and quantum computation [7–9]. Another important application of entanglement is the remote implementation of an operator (RIO), useful for distributed computation and network communication. The notion of RIO was first introduced by Huelga and collaborators in [20], where Bob possesses an unknown unitary operator U and wishes to apply it to an arbitrary unknown state $|\psi\rangle$ held by Alice at a distant location via local operations and classical communication (LOCC). The point is that Alice does not know U and Bob does not know $|\psi\rangle$. The straightforward method to achieve this task is through double quantum state teleportation (DQST), which goes as follows: Alice first teleports her state $|\psi\rangle$ to Bob, Bob applies U to transform $|\psi\rangle$ to $|\psi'\rangle = U|\psi\rangle$ and then teleports $|\psi'\rangle$ back to Alice. For the qubit case, this costs a maximum of 2 ebits (i.e., entanglement bits measured by number of Einstein-Podolsky-Rosen maximally entangled pairs) and 4 cbits (i.e., traditional classical bits). However, Huelga *et al.* [21] demonstrated that RIO can be performed more efficiently using 2 ebits and only 3 cbits, reducing classical resources. They also devised a nontrivial protocol that uses minimal resources but succeeds only 50% of the time for a general 2×2 operator. Remarkably, for certain restricted sets of operators, RIO can be completed with 1 ebit and 2 cbits with a 100% success rate, making it more efficient than the straightforward DQST method [22]. Building on the work of Huelga's group, a lot of research teams have further investigated various facets of this problem, employing diverse forms of quantum entanglement to deepen the understanding of the topic [23–35]. Other variants of RIO, known as controlled remote implementation of operator (CRIO) [28,30,36–39,59], joint remote implementation of operator (JRIO) [40], controlled-joint remote implementation of operator (CJRIO) [41]. Hierarchical controlled joint remote implementation of operator (HCJRIO) [42] has also attracted the attention of the community. In such modified versions of RIO, a supervisor or/and a co-implementer comes into the game.

A maximally entangled state is a quantum state in which the degree of nonclassical correlation is the highest possible for a given constituent subsystem. In contrast, a non-maximally entangled state is one in which a subsystem exhibits weaker quantum correlation than in maximally entangled states. Maximally entangled states are highly valuable for many quantum information processing tasks because they enable optimal performance. As

for non-maximally entangled states, they may appear, say, from imperfect sources thanks to asymmetric coupling strengths/unequal amplitudes in decay channels or by application of a non-unitary local operation during the preparation process. However, non-maximal entanglement may be preferred in certain scenarios [43–45], in which case it is intentionally produced. In particular, the motivation for using non-maximally entangled states has been explicitly highlighted in recent papers [46–48] in the context of the resource theories of multipartite entanglement and quantum nonlocality. The quantum entanglement of a two-qubit system is well quantified by a measure called concurrence [49–51]. Concurrence equals 1 for maximal entanglement and decreases as entanglement weakens. For multipartite systems, Genuine Multipartite Entanglement Measure (GMEM) [52–54] assesses the degree of entanglement across the entire system of multiple qubits, not just between pairs. Our protocol belongs to a class of global LOCC-based protocols that are quantumly controllable; as a rule, the controller (here, Charlie) must be entangled with the other participants (here, Alice and Bob), who are, in turn, quantumly correlated with each other. That genuine multipartite entanglement is necessary, and any biseparable states are irrelevant to such protocols. Yet, the degree of entanglement (here to be measured by the concurrence fill) plays a role in the resulting averaged non-conditioned fidelity, as will be elucidated later in section 3. Here, we adopt a GMEM for a three-qubit pure state, as defined in a recent paper by Xie and Eberly [52], called the concurrence fill $\mathbf{F}_{123}$, which is determined by the area of the so-called concurrence triangle. Namely,

$$\mathbf{F}_{123} = \left[\frac{16}{3} Q(Q - C^2_{1(23)})(Q - C^2_{2(13)})(Q - C^2_{3(12)})\right]^{\frac{1}{4}}, \tag{1}$$

where

$$Q = \frac{1}{2}[C^2_{1(23)} + C^2_{2(13)} + C^2_{3(12)}], \tag{2}$$

$$C^2_{i(jk)} = 2[1 - \mathrm{Tr}(\rho_i^2)] \quad \text{and} \quad \rho_i = \mathrm{Tr}_{jk}(|\Psi\rangle\langle\Psi|). \tag{3}$$

Here, $C_{i(jk)}$ denotes the concurrence value of subsystem i with the two remaining subsystems jk, $|\Psi\rangle$ is the three-qubit quantum state whose entanglement degree needs to be measured. Of course, the use of another entanglement measure changes the result quantitatively, but it is expected that the qualitative features remain similar to those obtained with the concurrence fill. In [43], the authors presented a probabilistic method for performing nonlocal operations on two qubits using a non-maximally entangled state, without converting it to a maximally entangled state first. In [55], a scheme was introduced for the controlled remote implementation of any arbitrary single-qubit operation by utilizing a non-maximally Greenberger-Horne-Zeilinger (GHZ) entangled state. In [32], a deterministic hierarchical quantum operation protocol was performed by using a five-qubit partially entangled state. Both protocols in [32,55] are implemented via the DQST method using maximal slice (MS) states [56] as quantum resources, thereby achieving a success probability of 100%. This is because Gao *et al.* [57] mathematically demonstrated that all states equivalent to MS states under local unitary transformations can be effectively utilized for perfect, deterministic controlled teleportation. Using real photons and hyperentanglement offers significant advantages for developing RIO compared with abstract qubits and conventional entanglement. A successful RIO involving single photons has been achieved using hyperentangled states and a cross-Kerr nonlinearity [58]. Recently, in Ref. [59], we designed three deterministic protocols for CRIO-related tasks using maximal

hyperentanglement. The first and second tasks focus on implementing operators on the photon state in S-DOF and P-DOF, respectively. The third task aims to perform the controlled remote implementation of a subset of operators on a photon that is simultaneously encoded in both S-DOF and P-DOF. Each of these tasks can be accomplished using a shared resource, specifically a GHZ hyperentangled state, which serves as the quantum resource.

This paper extends our previous work [59], in which a maximally hyperentangled state was used as the quantum resource, to the case of non-maximal hyperentanglement. The quantum hyperentanglement is deliberately set to a non-maximal value, with the channel parameters known exclusively to the controller. This enhances security by ensuring that no unauthorized party (Eve) can correctly manipulate Charlie's photon, even if Eve captures it. In this connection, it is worth reminding that when the channel is maximally hyperentangled, Eve can take over the control right if Charlie's photon is stolen, in which case Charlie's role as a controller is nullified. We show, in five explicit steps, that regardless of non-maximal shared hyperentanglement, the controller can still manage the CRIO to achieve unit fidelity, with a success probability that can also be controlled by tailoring the quantum channel parameters so that its concurrence satisfies eq. (1) remains less than but is close enough to one. More interestingly, we derive the average fidelity of classical protocols for the remote implementation of operators, then calculate the average non-conditioned fidelity to evaluate the degree of relevance of the quantum CRIO in terms of the so-called quantumness power and the controller's power.

The rest of this paper is composed of four more sections. Section 2 presents explicit steps to execute the CRIO using the quantum resource in the form of a tripartite state that is hyperentangled in both the S-DOF and P-DOF. The S-DOF part of the quantum resource is first used to convey the unknown coefficients of Alice's state to Bob. Then, after Bob applies his operator to his state, the P-DOF part of the quantum resource helps provide Alice with the desired state. As a consequence of non-maximal hyperentanglement of the quantum resource, the CRIO protocol is not deterministic, but, as a self-evident fact, its success probability can be made arbitrarily close to unity by engineering the parameters of the shared hyperentangled state. Section 3 is reserved for assessing the average non-conditioned fidelity of the RIO without the controller's participation, i.e., with Charlie's photon state traced out. Section 4 discusses some issues of interest. In this section, the criteria in terms of average classical CRIO fidelity (which is derived in the Appendix), average non-conditioned fidelity, and conditioned fidelity are established for the qualitative evaluation of a quantum CRIO protocol. For the quantitative purpose, the quantumness power, the controller's power, and the degree of relevance of the quantum CRIO are also defined. Section 5 concludes the paper.

2. Non-maximal hyperentanglement

In this paper, we consider only pure non-maximally entangled states. A pure non-maximally entangled state can be generated by an interaction dynamics strategy by which one starts from a product state and lets it time-evolve under a Hamiltonian to obtain a pure non-maximal entangled state in general at a given time. Pure non-maximally entangled states could also be obtained from pure maximally entangled ones. But in this case, one must use filtering by non-unitary operations or probabilistic LOCC, since local unitaries cannot change the Schmidt coefficients. Here, we are not interested in the details

of entanglement generation and right away consider a three-photon state of the following form

$$|Q^{(SP)}\rangle_{ABC} = |Q^{(S)}\rangle_{ABC}|Q^{(P)}\rangle_{ABC} \tag{4}$$

with

$$|Q^{(S)}\rangle_{ABC} = x|a_0\rangle_A|b_0\rangle_B|c_0\rangle_C + y|a_1\rangle_A|b_1\rangle_B|c_1\rangle_C, \tag{5}$$

$$|Q^{(P)}\rangle_{ABC} = z|H\rangle_A|H\rangle_B|H\rangle_C + t|V\rangle_A|V\rangle_B|V\rangle_C, \tag{6}$$

where the superscripts (P), (S) and (SP) indicate P-DOF, S-DOF alone and combined S-DOF and P-DOF, respectively, while $|H\rangle_{A(B,C)}$ ($|V\rangle_{A(B,C)}$) represents the horizontally (vertically) polarized state of photon $A(B, C)$ and $|a_0\rangle_A, |b_0\rangle_B, |c_0\rangle_C$ ($|a_1\rangle_A, |b_1\rangle_B, |c_1\rangle_C$) stand, respectively, for the state of photons A, B, C propagating along the spatial-path a_0, b_0, c_0 (a_1, b_1, c_1). The state (4) is a non-maximally hyperentangled GHZ-type state with real coefficients $0 < x, y, z, t < 1$ such that $x > y$, $z > t$, and $x^2 + y^2 = z^2 + t^2 = 1$. Using the entanglement measure from eq. (1), we can quantify the entanglement degree of the above states $|Q^{(S)}\rangle_{ABC}$ and $|Q^{(P)}\rangle_{ABC}$. For state $|Q^{(S)}\rangle_{ABC}$, the concurrence fill is $\mathbf{F}^{(S)}_{ABC} = 4x^2y^2$, whereas the concurrence fill of state $|Q^{(P)}\rangle_{ABC}$ is $\mathbf{F}^{(P)}_{ABC} = 4z^2t^2$. We shall demonstrate that the non-maximally hyperentangled state $|Q^{(SP)}\rangle_{ABC}$ could serve as a quantum resource for CRIO. Before continuing, we note that the state (4) must be prepared by Charlie. The process of generating such a hyperentangled state was described elsewhere in the literature (see, e.g., [60–62]). This guarantees that only Charlie knows the state parameters (4). As a rule, after preparation, Charlie should securely distribute the qubits A and B to Alice and Bob, respectively. Yet, for security reasons, the three parties must check whether Eve is present on the line by jointly examining the expected quantum correlations, say, by sending multiple states with decoy qubits inserted. The checking process is, in general, delicate and will not be described in detail here to save space. That is, we shall work with the state (4) assuming it was securely distributed among the three authorized parties.

We now set up the task to be executed. Alice has a photon a, whose quantum state is of the form

$$|\psi^{(SP)}\rangle_a = |\psi^{(S)}\rangle_a|V\rangle_a \tag{7}$$

with

$$|\psi^{(S)}\rangle_a = (\alpha|x_0\rangle + \beta|x_1\rangle)_a. \tag{8}$$

Here, photon a possesses a vertical polarization $|V\rangle$ and can simultaneously propagate along two spatial paths labelled x_0 and x_1. The coefficients α and β are unknown complex numbers satisfying the normalization condition $|\alpha|^2 + |\beta|^2 = 1$. Bob (a remote partner of Alice) has a general unitary operator $U^{(S)}$ which acts on the S-DOF and is represented by a 2×2 matrix with unknown complex elements u and v as

$$U^{(S)} = \begin{pmatrix} u & v \\ -v^* & u^* \end{pmatrix}. \tag{9}$$

Suppose that a future mission demands that Alice have a state determined by

$$|\psi_1^{(SP)}\rangle = U^{(S)}|\psi^{(SP)}\rangle = |\psi_1^{(S)}\rangle|V\rangle, \tag{10}$$

where

$$|\psi_1^{(S)}\rangle = (\alpha_1|x_0\rangle + \beta_1|x_1\rangle) \tag{11}$$

with

$$\alpha_1 = \alpha u - \beta v^*, \quad \beta_1 = \alpha v + \beta u^*. \tag{12}$$

The mission deems it so important that the process to provide Alice with the state (10) should be put under the control of a supervisor named Charlie, who will decide the completion of the task without the need to know either of the data α, β, u and v. Yet, the apparent trouble rests in the fact that Alice has no idea about u, v, and neither does Bob about α, β. We shall show that such a CRIO protocol can be done via the non-maximally hyperentangled state (4) shared among Alice, Bob, and Charlie. For the reason to be clarified later, here it is assumed that the coefficients x, y, z, t of the quantum state $|Q^{(SP)}\rangle_{ABC}$ is known only to Charlie. We shall calculate the protocol success probability in dependence on the entanglement degree of the quantum resource. For that purpose, let photons A, B, and C of the state (4) be allocated to Alice, Bob, and Charlie, respectively. The initial total state $|\psi^{(SP)}\rangle_a|Q^{(SP)}\rangle_{ABC}$ can be re-written as

$$|\psi^{(SP)}\rangle_a|Q^{(SP)}\rangle_{ABC} = |\Psi^{(S)}\rangle_{aABC}|V\rangle_a|Q^{(P)}\rangle_{ABC} \tag{13}$$

with

$$\begin{aligned}|\Psi^{(S)}\rangle_{aABC} = |\psi^{(S)}\rangle_a|Q^{(S)}\rangle_{ABC} = \alpha x|x_0\rangle_a|a_0\rangle_A|b_0\rangle_B|c_0\rangle_C + \alpha y|x_0\rangle_a|a_1\rangle_A|b_1\rangle_B|c_1\rangle_C \\ + \beta x|x_1\rangle_a|a_0\rangle_A|b_0\rangle_B|c_0\rangle_C + \beta y|x_1\rangle_a|a_1\rangle_A|b_1\rangle_B|c_1\rangle_C.\end{aligned} \tag{14}$$

For the CRIO protocol, we will carry out the following five steps in sequence:

Step 1: In this step, the operations only involve the S-DOF states, so we focus solely on the component $|\Psi^{(S)}\rangle_{aABC}$, while the P-DOF part of the quantum resource is omitted for a while. Alice is the first to work. She will carry out two types of work as shown in the left part of figure 1. Alice's first type of work is to take a coherent state (CS), denoted as $|z\rangle_d$, which has a positive real amplitude z and propagates along the path d, and let this CS interact with states $|x_0\rangle_a$ and $|a_0\rangle_A$ via the cross-Kerr mechanism with parameters θ and $-\theta$, respectively. The cross-Kerr mechanism is a nonlinear interaction that shifts the phase of one CS based on the presence of another CS. In particular, for a Fock state $|n\rangle$ and a CS $|z\rangle$, the cross-Kerr interaction with parameter θ transforms $|n\rangle|z\rangle$ to $|n\rangle|ze^{in\theta}\rangle$. After the nonlinear interactions, Alice performs a homodyne measurement on the resulting CS to determine its X-quadrature value. To perform this measurement, the to-be-measured CS as a probe mode is combined with a beam splitter with a local oscillator of the same frequency. The outputs are then detected using photodetectors. Provided the local oscillator is prepared in a large-amplitude CS with the same phase as the probe state, the homodyne measurement determines the value of an observable associated with the X-quadrature operator $\hat{X} = c + c^+$, with $c^+(c)$ the photon creation (annihilation) operator of the CS. By virtue of the explicit expression of the eigenstate $|X\rangle$ of $\hat{X}$, it can be shown that finding the quadrature value near $2z\cos(k\theta)$ implies that CSs $|ze^{\pm ik\theta}\rangle$ were measured. Note that the X-quadrature measurement cannot distinguish between the two CSs $|ze^{+ik\theta}\rangle$ and $|ze^{-ik\theta}\rangle$ for $k \neq 0$. Here, if the homodyne measurement outcome is $k = 0$ or $k = 1$, corresponding

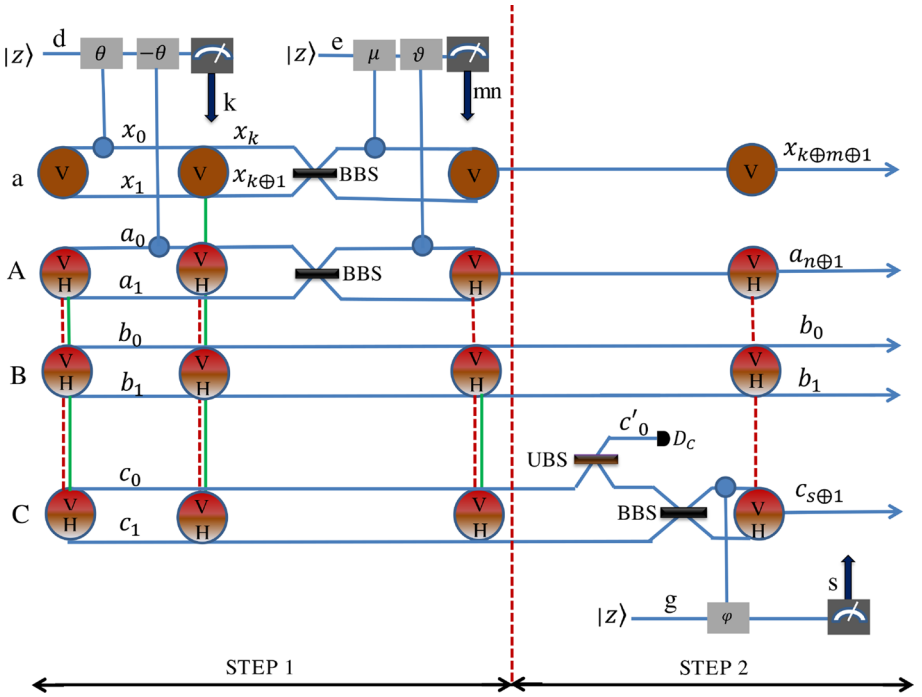


Figure 1. Actions of Alice in Step 1 and Charlie in Step 2 of the CRIO protocol utilizing a non-maximally hyperentangled GHZ state. A circle with two attached lines represents a photon propagating along two different paths simultaneously. In contrast, the letters 'V, H' inside a circle indicate a photon being in a superposition state of vertical $|V\rangle$ and horizontal $|H\rangle$ polarization. The symbols $\pm\theta$, μ, ν, φ represent the parameters of cross-Kerr interactions. Solid (dashed) lines connect photons entangled in S-DOF (P-DOF). Bold arrows represent classical communication channels used to transmit measurement results, and letters such as k, mn, and s indicate specific quantum measurement outcomes. BBS is a balanced beam splitter, while UBS is an unbalanced beam splitter with a reflection coefficient of y/x.

to the finding $|z\rangle$ or $|ze^{\pm i\theta}\rangle$, the state of the four photons collapses into

$$|T_k^{(S)}\rangle_{aABC} = N_k[xg_k|x_k\rangle_a|a_0\rangle_A|b_0\rangle_B|c_0\rangle_C + yg_{k\oplus 1}|x_{k\oplus 1}\rangle_a|a_1\rangle_A|b_1\rangle_B|c_1\rangle_C] \tag{15}$$

with a probability

$$P_k^{(S)} = N_k^{-2}, \tag{16}$$

where

$$N_k = [x^2|g_k|^2 + y^2|g_{k\oplus 1}|^2]^{-1/2}, \tag{17}$$

with $g_0 = \alpha$, $g_1 = \beta$ and $\oplus$ an addition mod 2. Inspecting states (14) and (15) reveals that the coefficients α and β of photon a have been embedded into the entangled state of the four photons a, A, B and C. The second type of work of Alice, in this step, is somewhat reverse to the first one, aiming to disentangle photon a and photon A from the two remaining photons B and C. To achieve this, Alice first performs an interference

experiment by sending two modes $|x_k\rangle_a$ and $|x_{k\oplus1}\rangle_a$ of photon a through a balanced beam splitter (BBS), and also simultaneously sending two modes $|a_0\rangle_A$ and $|a_1\rangle_A$ of photon A through another BBS. Subsequently, Alice uses a different CS $|z\rangle_e$ and activates the cross-Kerr mechanism with interaction parameters μ and ν with the modes $|x_k\rangle_a$ and $|a_0\rangle_A$, respectively. After the nonlinear interactions, Alice performs a homodyne measurement on the resulting CS to determine its phase associated with the found X-quadrature value. The homodyne measurement may detect a CS $|ze^{i(m\mu+n\nu)}\rangle_e$ for $m, n \in \{0, 1\}$. If the measurement outcome is $mn \in \{00, 01, 10, 11\}$, the four photons are projected onto the state

$$|\Lambda^{(S)}_{kmn}\rangle_{aABC} = N_k|x_{m\oplus k\oplus1}\rangle_a|a_{n\oplus1}\rangle_A\Big[xg_k|b_0\rangle_B|c_0\rangle_C + (-1)^{m\oplus n\oplus k}yg_{k\oplus1}|b_1\rangle_B|c_1\rangle_C\Big]. \tag{18}$$

The probability $P^{(S)}_{mn}$ of obtaining state (18) from state (15) is one quarter for any possible pair of m and n. That is,

$$P^{(S)}_{mn} = \frac{1}{4}. \tag{19}$$

After Step 1, the photons a and A are separated in the S-DOF from the photons B and C, while all four photons remain entangled in the P-DOF. Note that, since the state of photon a is completely separated from the other photons, we can disregard that photon from now on, as it no longer plays a role in the next steps.

Step 2: This step is a little bit tricky and illustrated in the right part of figure 1 and manipulated by Charlie, who knows the parameters x and y. First, Charlie uses an unbalanced beam splitter (UBS) with a reflection coefficient equal to y/x (recall that we assumed a non-maximally entangled state with parameters $x > y$ and $z > t$) placed in mode c_0. After passing the UBS, the state of photons A, B and C becomes

$$|Y^{(S)}_{kmn}\rangle_{ABC} = N_k\Big[y|\Gamma^{(S)}_{kmn}\rangle_{ABC} + \sqrt{x^2-y^2}g_k|a_{n\oplus1}\rangle_A|b_0\rangle_B|c'_0\rangle\Big] \tag{20}$$

with

$$|\Gamma^{(S)}_{kmn}\rangle_{ABC} = |a_{n\oplus1}\rangle_A\Big[g_k|b_0\rangle_B|c_0\rangle_C + (-1)^{m\oplus n\oplus k}g_{k\oplus1}|b_1\rangle_B|c_1\rangle_C\Big]. \tag{21}$$

Charlie then uses a detector D_C to detect photon in path c'_0. If photon C is detected there, the CRIO protocol fails. Otherwise, if the photodetector does not detect any photon in path c'_0, the state of photons A, B and C is left as $|\Gamma^{(S)}_{kmn}\rangle_{ABC}$ with a probability

$$P^{(S)}_D = y^2N_k^2. \tag{22}$$

Second, Charlie needs to disentangle photon C from photon B in the S-DOF. To do this, she uses a BBS to mix mode c_0 and mode c_1, followed by turning on the interaction between mode c_k and a CS $|z\rangle_g$ via cross-Kerr mechanism with parameter φ. Afterward, Charlie measures the X-quadrature of the CS. The measurement outcome may be $s = 0$ if the CS is found in $|z\rangle_g$ or $s = 1$ if the CS is found in $|ze^{\pm i\varphi}\rangle_g$. Explicitly, obtaining an outcome s projects the S-DOF state of photons A, B and C onto

$$|\Theta^{(S)}_{kmns}\rangle_{ABC} = |a_{n\oplus1}\rangle_A\Big[g_k|b_0\rangle_B + (-1)^{m\oplus n\oplus k\oplus s}g_{k\oplus1}|b_1\rangle_B\Big]|c_{s\oplus1}\rangle_C \tag{23}$$

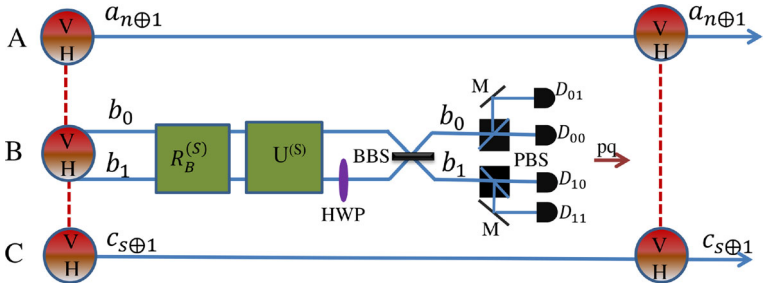


Figure 2. Bob's actions in Step 3 of the CRIO protocol. HWP is a half-wave plate which changes the polarization of a photon, PBS is a polarization beam splitter, M is a mirror, and D_{pq} are photodetectors. The operator $U^{(S)}$ is defined in eq. (9) and $R_B^{(S)} = X_S^k Z_S^{k\oplus m\oplus n\oplus s}$.

with a probability

$$P_s^{(S)} = \frac{1}{2}. \tag{24}$$

As is clear from eq. (23), the coefficients α and β in the state of photon a have been transferred to the state of photon B. The total probability to obtain the state (23) above is

$$P^{(S)} = \sum_{k,m,n,s=0}^{1} P_k^{(S)} P_{mn}^{(S)} P_D^{(S)} P_s^{(S)} = 2y^2. \tag{25}$$

Step 3: Bob shows up in this step with his actions displayed in figure 2. Namely, after receiving through a classical communication channel (which must be reliable but not necessarily secure) the outcomes k, m, n announced by Alice and s by Charlie, he first applies on photon B the operator $R_B^{(S)} = X_S^k Z_S^{k\oplus m\oplus n\oplus s}$, with $X_S = |b_0\rangle_B\langle b_1| + |b_1\rangle_B\langle b_0|$ and $Z_S = |b_0\rangle_B\langle b_0| - |b_1\rangle_B\langle b_1|$, and then implements the operator $U^{(S)}$ in eq. (9) on photon B, to obtain

$$|\chi_{ns}^{(S)}\rangle_{ABC} = |a_{n\oplus1}\rangle_A(\alpha_1|b_0\rangle_B + \beta_1|b_1\rangle_B)|c_{s\oplus1}\rangle_C, \tag{26}$$

with α_1, β_1 given by (12). Now, it is time to 'transport' the coefficients α_1, β_1 of Bob's photon state to the state of Alice's photon without transporting photon B itself in any real way. Such a 'quantum transportation' is aided by the P-DOF part of the quantum resource. Thus, we have to deal with the full state of the three photons A, B, and C with the P-DOF added, which reads

$$|\Omega_{ns}^{(SP)}\rangle_{ABC} = |\chi_{ns}^{(S)}\rangle_{ABC}|Q^{(P)}\rangle_{ABC}. \tag{27}$$

Bob places on path b_1 a half-wave plate (HWP), which flips the polarization state as $|H\rangle_B \rightleftarrows |V\rangle_B$. He then mixes the two states $|b_0\rangle_B$ and $|b_1\rangle_B$ on a BBS, followed by two polarization beam splitters (PBSs) and four photodetectors D_{pq}, with $p, q \in \{0, 1\}$, to identify properties of the outgoing photon B. Since a PBS transmits horizontal polarization and reflects vertical polarization, and only one detector can click, detailed calculations yield the following results.

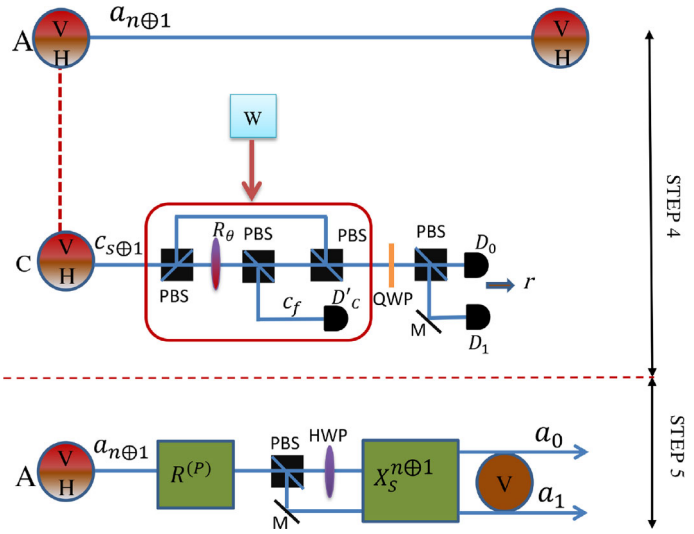


Figure 3. Charlie's actions in Step 4 and Alice's actions in Step 5 of the CRIO protocol. W is a device system which includes three PBSs, one wave plate R_θ and one photon detector D'_C. R_θ is a wave plate, which is used to rotate the horizontal polarization with an angle $\theta = \arccos(t/z)$. QWP is the R_θ with $\theta = \pi/4$.

The probability $P_{pq}^{(P)}$ that detector D_{pq} with any possible p, q clicks are found to be dependent only on q, i.e.,

$$P_{pq}^{(P)} = \frac{1}{2} M_q^{-2}, \tag{28}$$

where

$$M_q = (z^2|h_q|^2 + t^2|h_{q\oplus1}|^2)^{-1/2} \tag{29}$$

with $h_0 = \alpha_1$, $h_1 = \beta_1$. When D_{pq} clicks state (27) is collapsed into

$$|\Pi_{nspq}^{(SP)}\rangle_{AC} = M_q|a_{n\oplus1}\rangle_A[zh_q|H\rangle_A|H\rangle_C + (-1)^p th_{q\oplus1}|V\rangle_A|V\rangle_C]|c_{s\oplus1}\rangle_C. \tag{30}$$

As is obvious from the eq. (30), photons A and C remain entangled in the P-DOF. No one except Charlie, who is capable of disentangling them in such a way that the coefficients α_1, β_1 belong to photon A only. Actually, Charlie's actions are displayed in the upper part of figure 3 and detailed in Step 4.

Step 4: First, Charlie uses the devices in box W which contains three PBSs, one wave plate R_θ with $\theta = \arccos(t/z)$ and one detector D'_C. Then, she in addition uses one-quarter wave plate (QWP), one more PBS, and two more detectors D_r with $r = 0$ and $r = 1$. The wave plate R_θ brings $|H\rangle$ ($|V\rangle$) to $\cos\theta|H\rangle + \sin\theta|V\rangle$ ($\cos\theta|V\rangle - \sin\theta|H\rangle$), and the QWP is nothing else but $R_{\pi/4}$. By straightforward calculations, it follows that, after passing all the devices but still before the detectors, state $|\Pi_{nspq}^{(SP)}\rangle_{AC}$ in eq. (30) will get the form

$$|L_{nspq}^{(SP)}\rangle_{AC} = M_q\{\sqrt{z^2 - t^2}h_q|a_{n\oplus1}, H\rangle_A|c_f, V\rangle_C + \frac{t}{\sqrt{2}}[(h_q|a_{n\oplus1}, H\rangle_A + (-1)^p h_{q\oplus1}$$

$$\times |a_{n\oplus 1}, V\rangle_A)|c_{s\oplus 1}, H\rangle_C + (h_q|a_{n\oplus 1}, H\rangle_A - (-1)^p h_{q\oplus 1}|a_{n\oplus 1}, V\rangle_A)|c_{s\oplus 1}, V\rangle_C]\}. \tag{31}$$

If D'_C does not fire and D_r does, then for whatever $r \in \{0, 1\}$ (to be publicly published), the above state collapses into

$$|\Sigma^{(SP)}_{npqr}\rangle_A = |a_{n\oplus 1}\rangle_A(h_q|H\rangle_A + (-1)^{p+r} h_{q\oplus 1}|V\rangle_A) \tag{32}$$

with a probability

$$P^{(P)}_r = \frac{1}{2}t^2 M_q^2. \tag{33}$$

The total probability of getting state (32) from state (27) is

$$P^{(P)} = \sum_{p,q,r=0}^{1} P^{(P)}_{pq} P^{(P)}_r = 2t^2. \tag{34}$$

Clearly, state (32) can solely be manipulated by Alice. But, until this moment, it has not yet been in the exact form of the desired one. To complete the CRIO, Alice must act as described in Step 5 (see also the lower part of figure 3).

Step 5: Alice first manipulates the P-DOF part of state (32). She applies on photon A the operator $R^{(P)} = X_P^q Z_P^{p\oplus r}$, with $X_P = |H\rangle_A\langle V| + |V\rangle_A\langle H|$ and $Z_P = |H\rangle_A\langle H| - |V\rangle_A\langle V|$, which transforms state (32) to state $|a_{n\oplus 1}\rangle_A \otimes (\alpha_1|H\rangle_A + \beta_1|V\rangle_A)$. She next manipulates the S-DOF of that state by applying on it the operators PBS, HWP and $X_S^{n\oplus 1}$ in sequence. The resulting state becomes precisely the desired one, i.e., the state $|\psi_1^{(SP)}\rangle$ in eq. (10).

3. Non-conditioned fidelity

The role of the controller, Charlie, is obvious: with her active assistance, Alice and Bob can collaborate towards providing Alice with a replica of state $|\psi_1^{(SP)}\rangle = U^{(S)}|\psi^{(SP)}\rangle$ of eq. (10). In this connection, it makes sense to ask a question like this: Could Alice and Bob still collaborate somehow without Charlie's participation to prepare for Alice a state that though is not 100% coincident with but close to $|\psi_1^{(SP)}\rangle$? And, the point is, how close is it attainable?

Let us calculate the so-called non-conditioned fidelity of the CRIO, which is the fidelity obtained when the controller Charlie stands outside the game, while her quantum correlations with Alice and Bob are preserved. Such a scenario was investigated intensively in controlled quantum teleportation [64–72].

Recall that after Alice's actions described in Step 1 of the previous section, with a probability of $P^{(S)}_{kmn} = \frac{1}{4}N_k^{-2}$, the whole system is projected onto the state $|\Lambda^{(S)}_{kmn}\rangle_{aABC}|Q^{(P)}\rangle_{ABC}$, with $|\Lambda^{(S)}_{kmn}\rangle_{aABC}$ and $|Q^{(P)}\rangle_{ABC}$ given in eqs (18) and (6), respectively. Despite Charlie's non-participation, Bob continues the job by first applying $U^{(S)}X_S^k Z_S^{k\oplus m\oplus n}$ on photon B, then using one HWP, one BBS, four PBSs and four photodetectors D_{pq} with $p, q \in \{00, 01, 10, 11\}$ (see the right part of figure 2) to detect photon B with its certain spatial path and polarization. When a photodetector D_{pq} fires,

with a probability of $P_{pq}^{(P)} = \frac{1}{2}N_k^2 M_{kq}^{-2}$, the system state collapses into

$$|R_{knpq}^{(SP)}\rangle_{AC} = M_{kq}|a_{n\oplus 1}\rangle_A\Big[\alpha f_k(zw_q|H\rangle_A|c_k, H\rangle_C + (-1)^p t w_{q\oplus 1}|V\rangle_A|c_k, V\rangle_C) - (-1)^q \beta f_{k\oplus 1}(zw_{q\oplus 1}^*|H\rangle_A|c_{k\oplus 1}, H\rangle_C - (-1)^p t w_q^*|V\rangle_A|c_{k\oplus 1}, V\rangle_C)\Big], \tag{35}$$

where

$$M_{kq} = [z^2(f_k^2|\alpha w_q|^2 + f_{k\oplus 1}^2|\beta w_{q\oplus 1}|^2) + t^2(f_k^2|\alpha w_{q\oplus 1}|^2 + f_{k\oplus 1}^2|\beta w_q|^2)]^{-1/2} \tag{36}$$

with $f_0 = x$, $f_1 = y$, $w_0 = u$ and $w_1 = v$. Finally, Alice applies in sequence $X_P^q Z_P^p$, one PBS, one HWP and $X_S^{n\oplus 1}$ to photon A as depicted in the right part of her actions in figure 3, recasting $|R_{knpq}^{(SP)}\rangle_{AC}$ to a state in which the tracing photon C results in a mixed state of photon A as

$$\rho_A(k,q) = M_{kq}^2[z^2(f_k^2|\alpha w_q|^2 + f_{k\oplus 1}^2|\beta w_{q\oplus 1}|^2)|a_q\rangle_A\langle a_q| + t^2(f_k^2|\alpha w_{q\oplus 1}|^2 + f_{k\oplus 1}^2|\beta w_q|^2)|a_{q\oplus 1}\rangle_A\langle a_{q\oplus 1}|]|V\rangle_A\langle V|. \tag{37}$$

The closeness between the mixed state $\rho_A(k,q)$ and the desired pure state $|\psi_1^{(SP)}\rangle$ is assessed by the non-conditioned fidelity $F_{NC}(k,q) = \langle\psi_1^{(SP)}|\rho_A(k,q)|\psi_1^{(SP)}\rangle$. The Straightforward calculation gives

$$F_{NC}(k,q) = M_{kq}^2[z^2(f_k^2|\alpha w_q|^2 + f_{k\oplus 1}^2|\beta w_{q\oplus 1}|^2)|h_q|^2 + t^2(f_k^2|\alpha w_{q\oplus 1}|^2 + f_{k\oplus 1}^2|\beta w_q|^2)|h_{q\oplus 1}|^2], \tag{38}$$

where $h_0 = \alpha_1$ and $h_1 = \beta_1$. The above non-conditioned fidelity is not universal in the sense that it depends on both Alice's initial state via the coefficients $\{\alpha, \beta\}$ and Bob's operator via the parameters $\{u, v\}$. In a situation like this, one should average over all input states and all input operators to get the average non-conditioned fidelity $\bar{F}_{NC}(k,q)$, which is determined by

$$\bar{F}_{NC}(k,q) = \int \mathcal{D}\psi \int \mathcal{D}U\, F_{NC}(k,q) \tag{39}$$

with $\mathcal{D}\psi$ ($\mathcal{D}U$) a measure of the input state (the input operator) distribution. Let us adopt the following parametrization: $\alpha = \cos\vartheta$, $\beta = e^{i\xi}\sin\theta$, $u = \cos\gamma$, $v = e^{i\delta}\sin\gamma$ with $0 \le \xi, \delta \le 2\pi$ and $0 \le \vartheta, \gamma \le \pi/2$. Then, assuming all states and operators appear equally often, one has

$$\mathcal{D}\psi = \frac{1}{2\pi}\sin(2\vartheta)d\vartheta d\xi \tag{40}$$

and

$$\mathcal{D}U = \frac{1}{2\pi}\sin(2\gamma)d\gamma d\delta. \tag{41}$$

At this point, we look more closely at eq. (38) which discloses

$$F_{NC}(0,1)|_{u\rightleftarrows v,\alpha_1\rightleftarrows\beta_1} = F_{NC}(1,1)|_{u\rightleftarrows v,\alpha_1\rightleftarrows\beta_1,x\rightleftarrows y} = F_{NC}(0,0) = F_{NC}(1,0)|_{x\rightleftarrows y}. \tag{42}$$

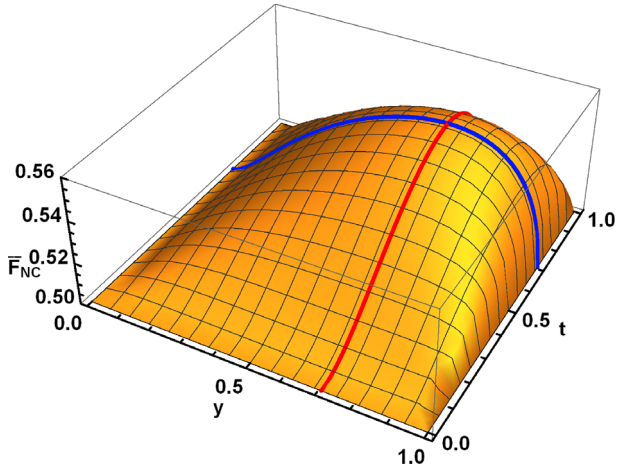


Figure 4. Average non-conditioned fidelity $\bar{F}_{NC}$ as function of the parameters y and t of the working quantum channel. The red (blue) curve is the average non-conditioned fidelity as a function of $t\,(y)$ for $y(t) = 1/\sqrt{2}$. The two curves (red and blue) intersect at $\bar{F}_{NC} = 5/9$ when $x = y = z = t = 1/\sqrt{2}$, corresponding to maximal entanglement in both the S-DOF and the P-DOF. Although this figure plots $\bar{F}_{NC}$ over the full domain of $y, t \in [0, 1]$, only the region with $0 < y, t < 1/\sqrt{2}$ is relevant, in correspondence with our assumed conditions $y < x$ and $t < z$ mentioned in Step 2 below eq. (6).

Since the exchange $x \leftrightarrows y$ does not change the shape of the non-conditioned fidelity $F_{NC}(k, q)$ and the degree of entanglement of the quantum resource, while the exchanges $u \rightleftarrows v$ and $\alpha_1 \rightleftarrows \beta_1$ preserve the value of the average one, $\bar{F}_{NC}(k, q)$, it follows that $\bar{F}_{NC} = \bar{F}_{NC}(0, 0) = \bar{F}_{NC}(0, 1) = \bar{F}_{NC}(1, 0) = \bar{F}_{NC}(1, 1)$ (these equalities are indeed verified numerically). In figure 4, we draw a 3D plot of the average non-conditioned fidelity $\bar{F}_{NC}$ in dependence on the parameters y and t of the working quantum resource.

4. Discussion

The present CRIO employs a non-maximally hyperentangled quantum resource whose parameters are deliberately made known only to the controller, Charlie, and not to the system. This allows no one else, but Charlie, to choose an unbalanced beam splitter with the right reflection coefficient in Step 2, as well as a wave plate R_θ with the right value of θ in Step 4, for her proper actions. This also guarantees the protocol's security, in the sense that any other party that might capture qubit C cannot manipulate it correctly. Conditioned on the results of Charlie's measurements, Alice and Bob can complete the RIO with a replica of the desired state $U^{(S)}|\psi^{(SP)}\rangle$ at Alice's place. The price of using non-maximal hyperentanglement is a success probability <1. This can be justified by analyzing the protocol's total success probability $P^{(\text{Total})} = P^{(S)}P^{(P)} = 4y^2t^2$, with $P^{(S)}$ given by (25) and $P^{(P)}$ by (34). As assumed in section 2, $0 < x, y, z, t < 1$, $y < x$ and $t < z$. Then, combined with the normalization conditions $x^2 + y^2 = z^2 + t^2 = 1$, it follows that $y^2 < x^2 = 1 - y^2$ and $t^2 < z^2 = 1 - t^2$, which in turn imply $0 < y^2, t^2 < 1/2$. Such constraints on y^2 and t^2 justify the said statement. However, as is self-evident, the success probability can be brought arbitrarily close to 1 by tailoring the quantum resource with y

and t approaching but not equal to $1/\sqrt{2}$, i.e., by making the quantum resource closer and closer to the maximally hyperentangled one, but the degree of entanglement remains <1.

As for the relevance of the quantum CRIO, it can be evaluated by three quantities: The usual conditioned fidelity F_C (i.e., the one with the controller's cooperation), the average classical fidelity $\bar{F}_{Cl}$ (i.e., the one obtained solely by classical means after averaging over all possibilities for all operators U and all states $|\psi\rangle$ with uniform distributions) and the so-called average non-conditioned fidelity $\bar{F}_{NC}$ (i.e., the one without the controller's participation). We here adopt the following criteria: A quantum CRIO is relevant if and only if

$$F_C > \bar{F}_{Cl} > \bar{F}_{NC}. \tag{43}$$

Physically, the meanings of the above inequalities are the following. The first inequality signifies the advantage of the quantumness in the CRIO: The use of quantum resources (no matter whether it is maximally entangled or not) should surpass the use of any classical channels. The second inequality measures the controller's role: The quantum CRIO protocol without participation of the controller should not be as good as, or better than, the classical one; otherwise, the controlling function does not work. Based on the criteria (43), we say qualitatively that if $\bar{F}_{NC} \geq \bar{F}_{Cl}$ or/and $\bar{F}_{Cl} \geq F_C$ then the CRIO protocol appears irrelevant regarding both controlling meaning and quantum advantage. Quantitatively, we may interpret

$$QP = \max\left\{\frac{F_C - \bar{F}_{Cl}}{1 - \bar{F}_{Cl}}, 0\right\} \tag{44}$$

as the quantumness power,

$$CP = \max\left\{\frac{\bar{F}_{Cl} - \bar{F}_{NC}}{\bar{F}_{Cl} - \min \bar{F}_{NC}}, 0\right\} \tag{45}$$

as the controller's power and

$$\mathcal{R} = CP \times QP \tag{46}$$

as the degree of relevancy.

In our protocol $F_C = 1$ (in text) and $\bar{F}_{Cl} = 5/9$ (see appendix) so $QP = 1$ confirming the strongest quantum power. To assess the controller's power, we plot in figure 4 the average non-conditioned fidelity $\bar{F}_{NC}$ (see eq. 39) as a function of the hyperentanglement degree in terms of the parameters t and y. Inspecting figure 4 reveals that, for a fixed value of y, the average non-conditioned fidelity $\bar{F}_{NC}$ is first increasing with t for $t \in (0, 1/\sqrt{2}]$ and then decreasing with t for $t \in [1/\sqrt{2}, 1)$. Likewise, for a fixed value of t, $\bar{F}_{NC}$ is first increasing with y for $y \in (0, 1/\sqrt{2}]$ and then decreasing with y for $y \in [1/\sqrt{2}, 1)$. In other words, for a fixed degree of entanglement in S-DOF $\mathbf{F}^{(S)}_{ABC} = 4y^2\sqrt{1-y^2}$ (P-DOF $\mathbf{F}^{(P)}_{ABC} = 4t^2\sqrt{1-t^2}$), $\bar{F}_{NC}$ is proportional to the degree of entanglement in P-DOF (S-DOF). Remarkably, $\bar{F}_{NC}$ attains its highest value max $\bar{F}_{NC}$ which exactly equals 5/9 when $y = t = 1/\sqrt{2}$, corresponding to the maximal entanglement in both S-DOF and P-DOF (i.e., $\mathbf{F}^{(S)}_{ABC} = \mathbf{F}^{(P)}_{ABC} = 1$), whereas its lowest value min $\bar{F}_{NC}$ is about 1/2 when y or/and t is tending to 0 (1), corresponding to vanishing entanglement in S-DOF or/and P-DOF (i.e., with $\mathbf{F}^{(S)}_{ABC}$ or/and $\mathbf{F}^{(P)}_{ABC}$ approaching zero). Comparing $\bar{F}_{NC}$ with $\bar{F}_{Cl}$ and

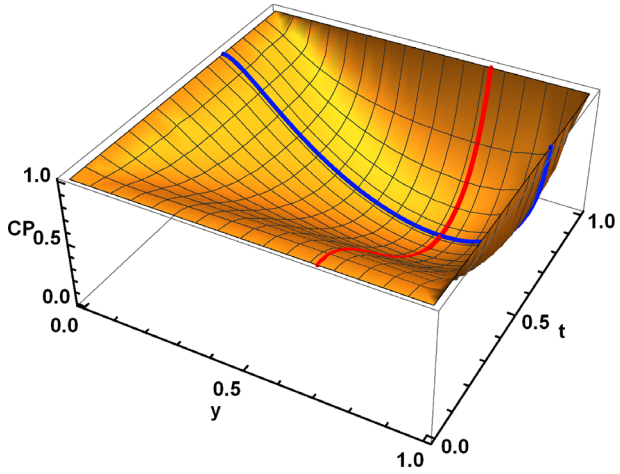


Figure 5. Controller's power CP as a function of the parameters y and t of the working quantum resource. The red (blue) curve is the controller's power as a function of $t\,(y)$ for $y(t) = 1/\sqrt{2}$. The two curves (red and blue) intersect at CP $= 0$ when $x = y = z = t = \frac{1}{\sqrt{2}}$, corresponding to maximal entanglement in both the S-DOF and the P-DOF. Like in figure 4, only the region with $0 < y, t < \frac{1}{\sqrt{2}}$ is relevant in this figure too.

taking into account the definition (45), we realize that the controller's power is stronger for a lesser degree of entanglement. Putting this another way around, when the entanglement degree is increasing the controller's power is becoming weaker and, in particular, when the entanglement is maximal ($\mathbf{F}^{(S)}_{ABC} = \mathbf{F}^{(P)}_{ABC} = 1$, $\bar{F}_{NC} = 5/9$) the controller looses all her power ($CP = 0$) in the sense that without her participation the protocol fidelity, which equals the average classical fidelity ($\bar{F}_{NC} = \bar{F}_{Cl} = 5/9$), is still achievable. From such a controller's power point of view, partial entanglement appears 'better' than maximal entanglement. For better visualization, we also plot the controller's power (CP) versus y and t in figure 5.

Finally, we highlight the priority of using hyperentanglement. If usual entanglements are used for the CRIO, six photons served for the quantum resource must be consumed, of which three photons form a tripartite entanglement for Alice to teleport her state $|\psi\rangle$ to Bob, and the other three photons form another tripartite entanglement for Bob to teleport $U|\psi\rangle$ back to Alice. Using hyperentanglement requires only three photons, thereby economizing the shared quantum resource and reducing overhead costs.

5. Conclusion

In conclusion, for the purpose of saving quantum resources, we have proposed using hyperentanglement for the controlled remote implementation of an operator. The saving is significant, since only three photons are required instead of six to build the quantum resource. This is because two different degrees of freedom, the S-DOF and the P-DOF, are simultaneously exploited for each photon. The working quantum resource may be partially hyperentangled with its parameters, which are known to the controller. Despite non-maximal hyperentanglement, the fidelity of our protocol is still unity as the controller

(but no one else) is always able to perform the right measurements on his/her photon. Although the success probability is in general less than <1, it can be made arbitrarily close to 100% by appropriately tailoring the parameters of the quantum resource state without degrading the security in the sense mentioned above. We have also described how to implement the classical remote operator and derived its average fidelity to be $\bar{F}_{Cl} = 5/9$ (see appendix). From the perspective of the relevance of a controlled quantum protocol under the criteria (43), we have defined the quantifiers: the quantumness power, the controller's power, and the degree of relevance. We have then shown that a non-maximally hyperentangled state is relevant for our quantum-controlled remote implementation of an operator, but the maximally hyperentangled one is not. In a subsequent work, we shall consider hyperentangled states other than the GHZ-type and examine which type of hyperentanglement is most efficient, from a certain point of view, for the quantum-controlled remote implementation of an operator. The effects of noise, higher dimensionality, and mixedness are worth exploring further.

Before ending, it should be noted that the core resource is entirely defined within a finite-dimensional Hilbert space spanned by 3 photons, each characterized by both spatial and polarization DOFs. To fulfill the task, a CV physical implementation is involved by invoking additional CV coherent states to exploit their cross-Kerr interactions with single-photon states. However, it should be acknowledged that such deterministic cross-Kerr interactions remain a severe experimental bottleneck even when the amplitudes of the coherent states are made large. It is hoped that experimentalists can overcome future difficulties with appropriate adaptive modifications.

Acknowledgements

This work is supported by the Vietnam Academy of Science and Technology under Grant No. VAST01.03/26-27.

Appendix: Classical RIO

In this Appendix, we outline how RIO can be performed classically (i.e., without sharing any kinds of entanglement or physically sending any qubits) and derive the average fidelity of such a classical RIO. To be compact in formulations, we shall use matrix formalism. The Appendix can stand independently, so let us recapitulate the task of interest. Alice holds a qubit in an unknown pure state

$$|\psi\rangle = \sum_{j=0}^{1} c_j |j\rangle, \tag{47}$$

where $\{c_j \in \mathcal{C}; j = 0, 1\}$ are normalized coefficients which Alice has no ideas about, while $|0\rangle$ and $|1\rangle$ are two orthonormal states of some basis. Bob, a distant party of Alice, is provided with a single 2×2 unitary operator U of the form

$$U = \sum_{k=0}^{1} \sum_{l=0}^{1} u_{kl} |k\rangle\langle l|, \tag{48}$$

with unknown coefficients $\{u_{kl} \in \mathcal{C}; kl = 00, 01, 10, 11\}$ satisfying the unitary condition of U. He can apply U once to an arbitrary qubit state available at his spot. The two parties are allowed only to create known qubits, perform local measurements, and exchange bits

via a classical channel. They should cooperate in such a way that, in the end, Alice would end up with a qubit in a state as close as possible to

$$U|\psi\rangle = \sum_{j=0}^{1} \alpha_j |j\rangle, \tag{49}$$

where

$$\alpha_j = \sum_{m=0}^{1} c_m u_{jm}. \tag{50}$$

Such a task, called classical RIO, would go as follows. To start with, Alice measures her qubit in some basis spanned by $\{|j\rangle;\ j = 0, 1\}$. With a probability

$$P_j = |c_j|^2 \tag{51}$$

she finds her qubit in a state $|j\rangle$ and sends a bit j to Bob is to inform him of her measurement outcome. Alice also lets Bob know the basis she used for her measurement. Based on Alice's information, Bob prepares a qubit in the state $|j\rangle$, then applies U to $|j\rangle$ to transform it to

$$U|j\rangle = \sum_{n=0}^{1} u_{nj} |n\rangle. \tag{52}$$

He continues by measuring the transformed qubit in the same basis as Alice's. Bob would observe his qubit in a state $|n\rangle$ ($n = 0$ or 1) with a probability

$$P_{jn} = |u_{nj}|^2, \tag{53}$$

in which case, he conveys the value of n to Alice via a classical channel.

Remember that Alice measured her original qubit in the unknown state $|\psi\rangle$ and destroyed it, i.e., projected it on a state $|j\rangle$, which is known to her. So, upon having heard Bob's measurement outcome n, Alice applies $|n\rangle\langle j|$ to $|j\rangle$ to transform it to $|n\rangle$, which is the final approximate state with regard to the target one $U|\psi\rangle$. The closeness between such state $|n\rangle$ and $U|\psi\rangle$ is assessed by the fidelity

$$F_n = |\langle n|U|\psi\rangle|^2 = |\alpha_n|^2. \tag{54}$$

The total fidelity F results from the averaging over all four possibilities with $jn = \{00, 01, 10, 11\}$ weighted by their probabilities. That is,

$$F = \sum_{j,n=0}^{1} P_j P_{jn} F_n. \tag{55}$$

Setting $c_0 = \cos\theta$, $c_1 = e^{i\xi} \sin\theta$, $u_{00} = u_{11} = \cos\gamma$, $u_{01} = -u_{10}^* = e^{i\delta} \sin\gamma$ and using the above-mentioned expressions of P_j, P_{jn} and F_n, we can carry out the sum (55) yielding

$$F = \frac{1}{8}[5 + \cos(4\theta) + 2\cos^2(2\theta)\cos(4\gamma) + \cos(\xi + \delta)\sin(4\theta)\sin(4\gamma)]. \tag{56}$$

Clearly, F is both $|\psi\rangle$- and U-sensitive, i.e., depends on concrete U and $|\psi\rangle$ specified by $\{\theta, \xi, \gamma, \delta\}$. In such situations, of interest is the fidelity $\bar{F}$ which is averaged over all the involved parameters in their spaces of variation. Namely, $\bar{F} = \int \mathcal{D}\psi \int \mathcal{D}U\, F$. Assuming uniform distributions of the parameters in their spaces, i.e., the Haar-measures, we have $\mathcal{D}\psi = \frac{1}{2\pi}\sin(2\theta)d\theta d\xi$ and $\mathcal{D}U = \frac{1}{2\pi}\sin(2\gamma)d\gamma d\delta$. We can then Haar-integrate F to get

$$\bar{F}_{Cl} = \int \mathcal{D}\psi \int \mathcal{D}U\, F = \frac{5}{9}. \tag{57}$$

In the above equation, we use the subscript Cl to emphasize that $\bar{F}_{Cl}$ is the average fidelity of classical RIO.

In this connection, we note that if Bob had an infinite number of identical U and were capable of multiple applications of it to different known qubit states, then he would 100% succeed in identifying U (i.e., in precisely determining its characteristic parameters u_{kl} with all possible $kl \in \{00, 01, 10, 11\}$ by quantum process tomography). If so, Bob sends Alice the values of $\{u_{kl}\}$ via classical communication. Hence, Alice will be in the position to reconstruct U at her location and to apply it to her state $|\psi\rangle$ to obtain the desired state $U|\psi\rangle$. In other words, quantum process tomography implies that classical means alone suffice to 'teleport' full information of any unknown unitary operator. However, in the context under consideration, U can be used only once, so the information gained by Bob from his local actions is far from sufficient to identify U. Actually, in this context, the average fidelity is almost zero.

To complete this Appendix, it is also worth reminding that if the goal is just that Bob (but not Alice as in our proposed task) ends up with a state close to the target state $U|\psi\rangle$ then, after Alice sends Bob a bit j signifying that the measurement on her qubit $|\psi\rangle$ results in a state $|j\rangle$ (which happens with a probability $|c_j|^2$), Bob prepares a qubit in the state $|j\rangle$ and applies U to it to have the final state $U|j\rangle$. The fidelity between that state $U|j\rangle$ and the target one $U|\psi\rangle$ is $f_j = |\langle j|U^+U|\psi\rangle|^2 = |\langle j|\psi\rangle|^2 = |c_j|^2$. Therefore, the total classical fidelity f, which is the one to be obtained by taking into account the weight of the outcome j, is given by $f = \sum_{j=0}^{1}|c_j|^2 f_j = \sum_{j=0}^{1}|c_j|^4 = \cos^4\theta + \sin^4\theta$. Its average value $\bar{f}_{Cl} = \int \mathcal{D}\psi f$ with $\mathcal{D}\psi$ being the Haar-measure is easily calculated to be $2/3$, which is in essence that of the classical teleportation of an unknown qubit state from Alice to Bob [73,74].

References

[1] E Schrödinger, *Naturwissenschaften* **23**, 807 (1935)
[2] M Born, *Physik im Wandel meiner Zeit* (Springer, Berlin, 1983) p. 228
[3] P G Kwiat, *J. Mod. Opt.* **44**, 2173 (1997)
[4] F G Deng, B C Ren and X H Li, *Sci. Bull.* **62**, 46 (2017)
[5] J T Barreiro, T C Wei and P G Kwiat, *Nat. Phys.* **4**, 282 (2008)
[6] S P Walborn, *Nat. Phys.* **4**, 268 (2008)
[7] X L Wang, X D Cai, Z E Su, M C Chen, D Wu, L Li, N L Liu, C Y Lu and J W Pan, *Nature* **518**, 516 (2015)

[8] T M Graham, H J Bernstein, T C Wei, M Junge and P G Kwiat, *Nat. Commun.* **6** 7185 (2015)
[9] M X Luo, H R Li, H Lai and X Wang, *Phys. Rev. A* **93** 012332 (2016)
[10] B P Williams, R J Sadlier and T S Humble, *Phys. Rev. Lett.* **118**, 050501 (2017)
[11] M Nawaz and M Ikram, *J. Phys. B* **51**, 075501 (2018)
[12] P Zhou, X F Jiao and S X Lv, *Quantum Inf. Process.* **17**, 298 (2018)
[13] X F Jiao, P Zhou, S X Lv and Z Y Wang, *Sci. Rep.* **9**, 4663 (2019)
[14] P Zhou and L Lv, *Quantum Inf. Process.* **19**, 283 (2020)
[15] F Z Wu, G J Yang, H B Wang, J Xiong, F Alzahrani, A Hobiny and F G Deng, *Sci. China Phys. Mech. Astron.* **60**, 120313 (2017)
[16] X M Hu, Y Guo, B H Liu, Y F Huang, C F Li and G C Guo, *Sci. Adv.* **4**, 9304 (2018)
[17] L Nemirovsky-Levy, U Pereg and M Segev, *Opt. Quant.* **2**, 165 (2024)
[18] M Wang and H Guo, *Opt. Laser Technol.* **169**, 110075 (2024)
[19] C H Bennett, G Brassard, C Crepeau, R Jozsa, A Peres and W K Wootters, *Phys. Rev. Lett.* **70**, 1895 (1993)
[20] S F Huelga, J A Vaccaro, A Chefles and M B Plenio, *Phys. Rev. A* **63**, 042303 (2001)
[21] S F Huelga, M B Plenio and J A Vaccaro, *Phys. Rev. A* **65**, 042316 (2002)
[22] G Y Xiang, J Li and G C Guo, *Phys. Rev. A* **71**, 044304 (2005)
[23] C P Yang and J Gea-Banacloche, *J. Opt. B: Quantum Semiclass. Opt.* **3**, 407 (2001)
[24] M Hillery, V Buzek and A Berthiaume, *Phys. Rev. A* **59**, 1829 (1998)
[25] D Collins, N Linden and S Popescu, *Phys. Rev. A* **64**, 032302 (2001)
[26] Y F Huang, X F Ren, Y S Zhang, L M Duan and G C Guo, *Phys. Rev. Lett.* **93**, 240501 (2004)
[27] A M Wang, *Phys. Rev. A* **74**, 032317 (2006)
[28] A M Wang, *Phys. Rev. A* **75**, 062323 (2007)
[29] N B An, *Phys. Lett. A* **364**, 198 (2007)
[30] Q B Fan and D D Liu, *Sci. China Phys. Mech. Astron.* **51**, 1661 (2008)
[31] H Z Situ and D W Qiu, *Quantum Inf. Process.* **10**, 609 (2011)
[32] J Y Peng, L Tang and Z Yang, *Quantum Inf. Process.* **22**, 265 (2023)
[33] J Y Peng and Y He, *Int. J. Theor. Phys.* **58**, 3065 (2019)
[34] M Liu, N Maihemuti and J Y Peng, *Phys. Scr.* **99**, 045109 (2024)
[35] S Kumar, K Gangwar and A Pathak, *Phys. Scr.* **99**, 115106 (2024)
[36] L B Chen, Y H Liu and H Lu, *Mod. Phys. Lett. B* **24**, 431 (2010)
[37] L B Chen, R B Jin, T Peng and H Lu, *Int. J. Mod. Phys. B* **25**, 2853 (2011)
[38] Y B Zhan, X W Li, P C Ma and J Shi, *Chin. Phys. B* **22**, 040306 (2013)
[39] Y H He, Q C Lu, Y M Liao, X C Qin, J S Qin and P Zhou, *Int. J. Theor. Phys.* **54**, 1726 (2015)
[40] N B An, *J. Phys. A: Math. Theor.* **55**, 395304 (2022)
[41] S Kumar, N B An and A Pathak, *Euro. Phys. J. D* **78**, 90 (2024)
[42] R Jing, Q Lan and P Zhou P, *Entropy* **26**, 857 (2024)
[43] B Groisman and B Reznik, *Phys. Rev. A* **71**, 032322 (2005)
[44] S Mozes, J Oppenheim and B Reznik, *Phys. Rev. A* **71**, 012311 (2005)
[45] M Horodecki, A Sen De, U Sen and K Horodecki, *Phys. Rev. Lett.* **90**, 047902 (2003)
[46] D Rosset, D Schmid and F Buscemi, *Phys. Rev. Lett.* **125**, 210402 (2020)
[47] D Schmid, T C Fraser, R Kunjwal, A B Sainz, E Wolfe and R W Spekkens, *Quantum* **7**, 1194 (2023)
[48] S B Ghosh, S R Chowdhury, G Kar, A Roy, T Guha and M Banik, *Phys. Rev. Lett.* **132**, 250205 (2024)
[49] R Horodecki, P Horodecki, M Horodecki and K Horodecki, *Rev. Mod. Phys.* **81** 865 (2009)
[50] O Gühne and G Tóth, *Phys. Rep.* **474**, 1 (2009)
[51] W K Wootters, *Phys. Rev. Lett.* **80**, 2245 (1998)
[52] S Xie and J H Eberly, *Phys. Rev. Lett.* **127**, 040403 (2021)
[53] W Dür, G Vidal and J I Cirac, *Phys. Rev. A* **62**, 062314 (2000)
[54] Z H Ma, Z H Chen, J L Chen, C Spengler, A Gabriel and M Huber, *Phys. Rev. A* **83**, 062325 (2011)
[55] J Y Lin, J G He, Y C Gao, X M Li and P Zhou, *Int. J. Theor. Phys.* **56**, 1085 (2017)

[56] C J Zhang, Y S Zhang, S Zhang and G C Guo, *Phys. Rev. A* **76**, 012334 (2007)
[57] T Gao, F L Yan and Y C Li, *Euro. Phys. Lett.* **84**, 50001 (2008)
[58] X F Jiao, P Zhou and S X Lv, *J. Opt. Soc. Am. B* **36**, 867 (2019)
[59] N B An and C T Bich, *J. Phys. A: Math. Theor.* **55**, 225307 (2022)
[60] J W Pan, D Bouwmeester, M Daniell, H Weinfurter and A Zeilinger, *Nature* **403**, 515 (2000)
[61] A G White, D F V James, P H Eberhard and P G Kwiat, *Phys. Rev. Lett.* **83**, 3103 (1999)
[62] V Sultanov, T Santiago-Cruz and M V Chekhova, *Opt. Lett.* **47**, 3872 (2022)
[63] B C Ren, F F Du and F G Deng, *Phys. Rev. A* **88**, 012302 (2013)
[64] X H Li and S Ghose, *Phys. Rev. A* **90**, 052305 (2014)
[65] X H Li and S Ghose, *Phys. Rev. A* **91**, 012320 (2015)
[66] K Jeong, J Kim and S Lee, *Phys. Rev.* A **93**, 032328 (2016)
[67] N V Hop, C T Bich and N B An, *Int. J. Theor*. Phys. **56**, 810 (2017)
[68] A Barasi'nski and J Svozilík, *Phys. Rev. A* **99**, 012306 (2019)
[69] T J Wang, G Q Yang and C Wang, *Phys. Rev. A* **101**, 012323 (2020)
[70] T J Wang and S Ghose, *New J. Phys.* **22**, 123046 (2021)
[71] N V Hop, *Quan. Inf. Process.* **22**, 135 (2023)
[72] A Garg, S Adhikari, *Eur. Phys. J. D* **78**, 64 (2024).
[73] S Popescu, *Phys. Rev. Lett.* **72**, 797 (1994)
[74] S Massar and S Popescu, *Phys. Rev. Lett.* **74**, 1259 (1995)

Springer Nature or its licensor (e.g. a society or other partner) holds exclusive rights to this article under a publishing agreement with the author(s) or other rightsholder(s); author self-archiving of the accepted manuscript version of this article is solely governed by the terms of such publishing agreement and applicable law.